

See discussions, stats, and author profiles for this publication at: <https://www.researchgate.net/publication/253514105>

Nitric acid and nitrogen dioxide flux measurements: a new application of tunable diode laser absorption spectroscopy

Article in Proceedings of SPIE - The International Society for Optical Engineering · October 1999

DOI: 10.1117/12.366448

CITATIONS

28

READS

177

5 authors, including:



Cassandra Volpe Hori
California Institute of Technology

10 PUBLICATIONS 226 CITATIONS

SEE PROFILE



Mark S Zahniser
Aerodyne Research, Inc.

285 PUBLICATIONS 10,670 CITATIONS

SEE PROFILE



Barry McManus
Aerodyne Research, Inc.

146 PUBLICATIONS 5,633 CITATIONS

SEE PROFILE



Steven C. Wofsy
Harvard University

635 PUBLICATIONS 64,170 CITATIONS

SEE PROFILE

Some of the authors of this publication are also working on these related projects:



Methane Clumped Isotopes [View project](#)



Fluxnet-Canada [View project](#)

Nitric Acid and Nitrogen Dioxide Flux Measurements: a New Application of Tunable Diode Laser Absorption Spectroscopy

Cassandra Volpe Horii^{*a}, Mark S. Zahniser^b, David D. Nelson^b, J. Barry McManus^b, Steven C. Wofsy^a

^aHarvard University, 20 Oxford Street, Cambridge, MA 02138

^bAerodyne Research, Inc., 45 Manning Road, Billerica, MA 01821

ABSTRACT

A dual tunable diode laser absorption spectrometer (TDLAS) for continuous field measurement of nitric acid and nitrogen dioxide eddy covariance fluxes is described and preliminary field results are presented. The dual TDLAS simultaneously measures nitric acid (HNO₃) and nitrogen dioxide (NO₂) by direct absorption spectroscopy over a long path enclosed in an astigmatic Herriott multipass cell. The technique provides sufficient precision and time response (200 ppt RMS in 1 second) needed to record ambient variations and deposition rates by the eddy-covariance method. Real-time fitting of the integrated spectra over multiple absorption features makes the system appropriate for continuous field measurements while retaining the highly selective quality of direct absorption measurements and minimizing potential interferences. This method also produces an absolute, spectroscopic determination of concentration within the multipass cell, eliminating the need for calibrated gas mixtures in the field.

A field intercomparison of HNO₃ measurements was carried out in the fall of 1996 in Boulder, CO. The TDLAS prototype performed well under a wide variety of conditions within its noise limits as compared to the NOAA Aeronomy Laboratory Chemical Ionization Mass Spectrometer (CIMS). This first intercomparison demonstrated the accuracy and adaptability of the technique to unattended field operations, although instrumental baseline drift in the prototype was exaggerated by a lack of active temperature control on the optical elements. Since 1996, the new dual TDLAS has been constructed with particular attention to temperature stability and has demonstrated a marked improvement in both short and long-term noise. Preliminary results are presented, along with plans for the extended deployment at the Harvard Forest long-term ecological research site in central Massachusetts.

Keywords: nitric acid (HNO₃), nitrogen dioxide (NO₂), eddy covariance flux, tunable diode laser absorption spectroscopy

1. INTRODUCTION

Nitrogen oxides play an important role in determining the photochemistry of the troposphere by controlling the formation of tropospheric ozone, affecting the concentration of the hydroxyl radical, and contributing to acid precipitation^{1,2}. Nitric acid is often the most abundant of the nitrogen oxide species and provides the dominant sink for NO_x through surface deposition. Nitrogen dioxide is one of the most important reactive nitrogen species since its photolysis is the primary source of ozone in the troposphere. The rate for photochemical production of ozone depends on the presence of nitrogen oxides, NO_x = NO + NO₂. Total reactive oxidized nitrogen, NO_y, is the effective atmospheric reservoir for NO_x and is frequently dominated by HNO₃ in the rural boundary layer^{3,4,5}. Conversion of NO_x radicals to HNO₃ and subsequent deposition is thought to be an important loss process for reactive nitrogen and an important sink for HO_x radicals, which participate in the oxidation of hydrocarbons to form ozone^{1,6}.

Recent improvements in instrumental methods for detecting HNO₃ and NO₂ allow ambient measurements with sufficient time resolution for direct measurement of deposition fluxes. Observations of concentrations and deposition rates for the most important radical (NO₂) and non-radical (HNO₃) components of tropospheric reactive nitrogen will provide new information on the mechanisms and rates for removal of nitrogen oxides during transit from source regions. Present analyses indicate that HNO₃ should be the major depositing species and that heterogeneous processes form a significant fraction of HNO₃⁷. The

* Correspondence: Email: cvh@io.harvard.edu; Telephone: 617-495-5361; Fax: 617-495-2768

deployment of the dual TDLAS will provide the first experimental checks on these hypotheses. In addition, NO_2 measurements will allow us to assess claims that direct deposition of NO_2 may be significant compared to HNO_3 deposition in the atmospheric boundary layer NO_y budget¹. The Harvard Forest deployment presents the first opportunity to implement a continuous, year-round study of the speciation of reactive nitrogen in the boundary layer at a northern mid-latitude, rural site. Seasonal effects, interannual variability, and other potentially important changes impacting production of ozone will thus be investigated in the kind of detail that only such a well-equipped and continuously-operated site, with extensive ancillary measurements, can provide.

Since 1990, the Harvard Forest facility has conducted continuous, year-round measurements of O_3 , NO , NO_2 , NO_y , and the dry deposition fluxes (by eddy correlation) of NO_y and O_3 , along with non-methane hydrocarbons (C2-C6) and a wide variety of tracers of anthropogenic pollution such as CO , CO_2 , CFCs, and SF_6 . Measurements of peroxyacetyl nitrate (PAN), another key species in the NO_y family, are beginning in concert with the deployment of the TDLAS HNO_3 and NO_2 instrument. The long-term measurements at the site have characterized the atmospheric chemistry, indicating 20-30% very clean background air and comparable occurrence of significant pollution, and have established CO and C_2H_2 as quantitative indicators of pollution influence. Issues of local and regional transport pertaining to the photochemistry of ozone have been extensively studied^{7,8}.

2. EXPERIMENTAL METHODS

2.1. Dual TDLAS instrument

Although a number of techniques exist for making separate measurements of ambient HNO_3 and NO_2 , the TDLAS method is best suited for making both measurements at a long-term, unattended field site. Unlike the filter pack and mist chamber methods which are capable of determining HNO_3 concentrations at rates of minutes to hours, the TDLAS has the fast time response (1 s) and high data rate (1 Hz or higher) needed for flux measurements above a forest canopy^{9,10}. The Chemical Ionization Mass Spectrometer (CIMS) technique has both the sensitivity and time resolution necessary to perform eddy covariance flux measurements of HNO_3 ^{11,12,13}; this technique shows great promise for resolving many of the reactive nitrogen partitioning questions in the upper troposphere via aircraft measurements^{14,15,16}. Typical CIMS calibration methods involve use of a permeation device to relate the number of counts to the actual concentration, but this approach does not provide a reliably stable standard. The TDLAS method, which determines absolute concentrations based on tabulated spectroscopic parameters, is preferable for long term monitoring at the Harvard Forest site. TDLAS instruments are also routinely employed for measurement of eddy covariance fluxes¹⁷. Early TDLAS measurements of HNO_3 and NO_2 were limited by a large-volume (28 L) cell, slower time response, inability to subtract background spectra, and low computational duty cycle¹⁸. The current dual TDLAS represents a new generation of instruments using this technique where these problems have been largely eliminated¹⁹.

Figure 1 shows the schematic layout of the dual-channel HNO_3 and NO_2 infrared spectrometer. The instrument consists of two main modules: the measurement apparatus, including the diode lasers, optics, detectors, and reduced pressure multi-pass cell; and an

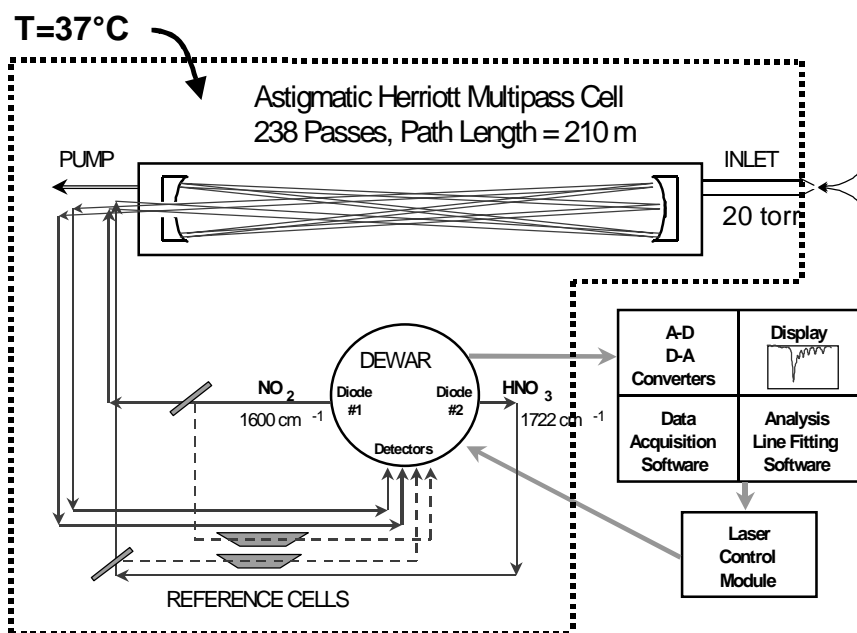


Figure 1. Schematic of the dual-channel TDLAS instrument.

electronics rack containing two Pentium computers running control and data acquisition software, and a two-channel laser temperature and current control unit (Laser Analytics, Inc.). The measurement apparatus is constructed on a two by four-foot aluminum optical table, surrounded by an aluminum shell, foam insulation, and a weatherproof polyethylene case. The aluminum shell and optical table form a conductive enclosure to which thin film Minco heaters are attached, allowing the temperature inside to be closely controlled. Based on an aircraft CO₂ instrument designed by B. Daube at Harvard²⁰, this design minimizes thermal gradients on the optical table which cause optical fringes to drift, adding noise and uncertainty to the measurements.

The dual TDLAS employs separate lead-salt diode lasers to produce distinct beams of two different frequencies corresponding to absorption lines for HNO₃ and NO₂ near 1720 cm⁻¹ and 1600 cm⁻¹ respectively. The diodes are operated close to threshold under single-mode conditions. A single liquid nitrogen dewar houses the two diodes along with the HgCdTe photovoltaic detectors for both the multi-pass cell sample beams and the reference cell beams.

The astigmatic Herriott absorption cell, developed at Aerodyne Research, Inc. (ARI), provides a long path length of 200 m or more in a volume of 5 liters²¹. The small volume of the cell insures a fast time response in the absence of wall effects. The sample gas is brought from atmospheric pressure to 20 torr across the inlet orifice in order to reduce the pressure broadening of the absorption lines, increasing the distinctive nature of the absorbing species' spectral signature. The inlet is heated to 30 C and designed so that the sample encounters only quartz or Pyrex that has been treated with a hydrophobic fluorinated silane coating in order to minimize surface interactions for "sticky" gases such as HNO₃. This coating has greatly improved the time response of the instrument to HNO₃ compared to uncoated Pyrex surfaces.

For a particular set of multi-pass cell dimensions, with fixed mirror radii of curvature and base length, there are distinct configurations of distance between and rotation of the mirrors for which the beam path exactly closes on itself and exits the cell through the coupling hole by which it entered. Within the range of an indexed adjustment fixture, the cell can be easily configured for a number of passes between approximately 100 and 350 by altering the mirror spacing and rotating the mirror axes. In practice, the longest possible pathlength with sufficient light transmission for optimal detection is selected. The instrument uses narrow-band dielectric mirror coatings with a reflectivity of 99.6% in the infrared. These mirrors provide sufficient transmission for 238 passes; with a base length of 88 cm, the total path length is 210 m in a volume of 5 liters. The pathlength is confirmed in the lab by observing the IR absorption of N₂O in both the 1600 and 1700 cm⁻¹ regions from standard additions into the multipass cell.

Once aligned, the multi-pass cell is quite insensitive to the aiming of the input beam. This allows two orthogonal beams to be multiplexed into the same cell, so that the separate patterns propagate through the cell with minimal interference. Two individual output beams emerge and are subsequently transmitted to separate detectors. In practice, a small amount of light from one beam is observed to scatter into the path of the second beam, but the intensity contributed by this light is 1% or less of the total observed intensity. The two diodes are modulated asynchronously so that the small cross-talk from the cell contributes only a negligible amount of random noise to the measurement. Figure 2 depicts a simulation of the beam reflections on the cell mirrors.

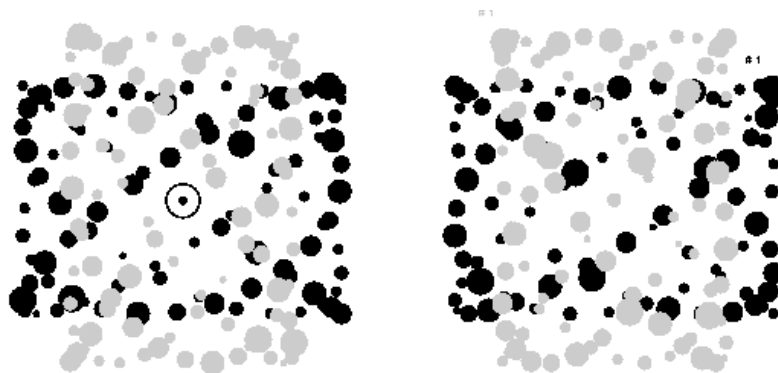


Figure 2. Calculated mirror beam spots for two patterns, each with 182 passes propagating in an astigmatic Herriott cell. The two different wavelengths are shown as different shades, and spot diameters are largest for the earliest reflections.

The TDLAS measures absorption spectra directly using rapid scan sweep integration, eliminating the need for second harmonic detection. Information on the unabsorbed laser power is retained, allowing direct, spectroscopic determination of concentration using predetermined line strengths, positions, and broadening coefficients. The result is an absolute measurement of the concentration of the trace gas. This spectroscopically derived concentration is routinely confirmed in the lab using calibrated HNO₃ permeation tubes and additions of NO₂ standards. The instrument does not require routine standard additions in the field.

The control module sweeps the current applied to the diodes in order to vary the wavelength over a number of absorption lines, typically 0.2 cm^{-1} , and acquire a distinctive “fingerprint” for the trace gas. Compared to monitoring at a single absorbing wavelength, this approach makes the retrieved concentrations less susceptible to potential interferences from other species absorbing in the same spectral region, as well as those of weak interference fringes inherent to the optical system. Fingerprint fits are performed with an iterative nonlinear least squares minimization routine which computes the Voigt profile for each line in the spectrum using the HITRAN spectral database line parameters²², temperature, and pressure in the cell. Figure 3 depicts a HNO_3 spectrum and the corresponding fingerprint fit.

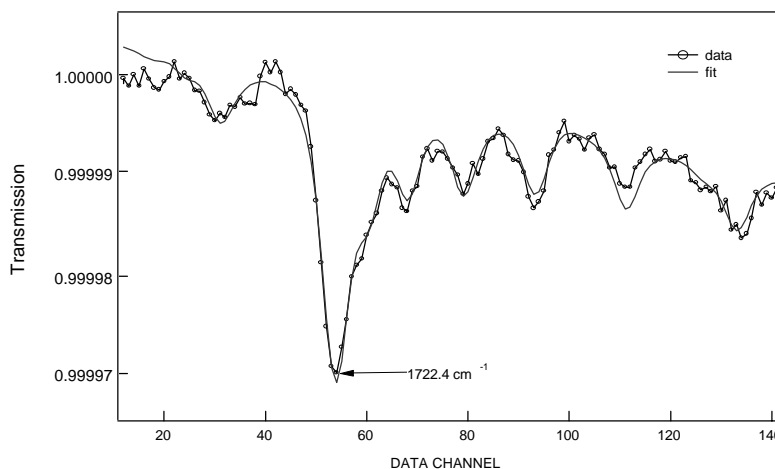


Figure 3. HNO_3 spectrum, 1722.3 cm^{-1} to 1722.5 cm^{-1} , 295 m path length, acquired during a field intercomparison in October 1996. 6 hours worth of 40-second spectra have been co-averaged and ratioed against an averaged background spectrum. The fit corresponds to 149 ppt HNO_3 .

The TDL software developed in QuickBasic at ARI runs in the DOS environment on two dedicated Pentium computers, one for each diode. TDL allows up to 45 individual lines to be used in the fingerprint fit for each species and can fit up to four species in each spectrum. The analysis of spectra is done in real time and resulting concentrations are saved to disk, with the option of archiving all raw spectra for later review or analysis. The TDL-95 Visual Basic program allows these computers to be installed in a remote location by providing access to all laser control, spectrum fitting, and data archiving functions over a phone line or via direct connection.

In order to further discriminate against non- HNO_3 and non- NO_2 spectral features, the flow is periodically modulated to remove the species of interest by creating a zone of scrubbed ambient air at the end of the inlet from which the flow is sampled to record a background spectrum. A nylon filter effectively removes ambient HNO_3 , and an activated charcoal filter in series removes ambient NO_2 . Laboratory and field tests show that four glass tubes positioned orthogonally around the tip of the inlet provide a >95% efficient means of delivery for the scrubbed ambient air under a wide range of conditions. This flow switching technique has the advantage of keeping a constant pressure within the cell, thus minimizing disturbance in the fringe field between signal and background spectra. The fine temperature control of the entire instrument also reduces the frequency required for background spectra to once every 15 minutes, allowing at least 80% of time in any half-hour flux interval to be spent measuring ambient concentrations at 1 Hz.

The dual TDLAS is readily adaptable to unattended, automated operation. Reference cells allow the system to lock onto the line positions of the species being measured so that the frequency, and therefore the measurement accuracy, does not drift over time. The diode and detector dewar is refilled automatically with liquid nitrogen using a temperature-sensing probe and triggered cryogenic solenoid valve. The system uses approximately 2 to 3 L LN_2 per day, depending on diode operating temperatures and currents.

2.2. Measurement of HNO_3

Determining absolute gas-phase nitric acid is complicated by its low concentrations in the troposphere (often less than 500 ppt) and the highly polar nature of the molecule which makes loss to sampling and inlet walls an important factor in any measurement technique. The TDLAS design minimizes adsorption of HNO_3 to the walls of the sampling cell by using a low-volume, high flow rate multi-pass cell with fluorinated silane coating (United Chemical Technologies compound #T2494) on the Pyrex inlet and flow cell walls. Once aged under ambient flow conditions, the coating reduces the degree of wall interaction for HNO_3 , as shown in Figure 4. A quartz flow tube performs similarly but does not require an aging period for the coating. With 80% of the HNO_3 time response described by a fast exponential (one second time constant), this technique provides an adequate method for measuring HNO_3 fluxes in the forest.

The inherent response function of the instrument to HNO_3 requires a small correction for the attenuation of fluxes carried by atmospheric eddies with frequencies higher than those detectable by the instrument; the correction procedure follows the established protocol for Harvard Forest NO_y fluxes. Munger et al.⁸ showed that the majority of NO_y fluxes at Harvard Forest are transported by eddies with frequencies between 0.005 and 0.5 Hz, with the peak of the power spectrum near 0.05 Hz. The existing NO_y detector at Harvard Forest has an exponential response function with a time constant of 1 second. For every half-hour period in which a flux is calculated, a response time correction factor is determined by numerically filtering the covariance of vertical wind and temperature (measured by a sonic anemometer coincident with the TDL inlet), $\langle w'T' \rangle$, by the response function of the instrument. The filtered $\langle w'T' \rangle$ is then compared to the unfiltered $\langle w'T' \rangle$ measurement to determine the percent of flux lost by attenuation of high frequency components. For NO_y this correction factor has been between 10 and 17%. During the day, however, the corrections tend to be smaller because the more turbulent daytime atmospheric boundary layer favors the larger, lower-frequency eddies. Since the TDLAS HNO_3 time response is 80% characterized by the same response function as the NO_y instrument, we expect to apply relatively small correction factors for the lost high-frequency flux components.

Previous measurements indicate that the NO_y flux at Harvard Forest varies from zero to $10 \mu\text{ moles m}^{-2} \text{ hr}^{-1}$, with a median July value of $4 \mu\text{ moles m}^{-2} \text{ hr}^{-1}$ ⁸. The sensitivity for HNO_3 flux is estimated as follows. The background noise of the HgCdTe photovoltaic detectors, the limited output power of the laser diodes, and the finite reflectivity of the multiple pass mirrors corresponds to approximately a precision of 80 ppt (peak absorbance of 1×10^{-5}) for HNO_3 in 1s. Actual noise is consistently 2 to 3 times higher due to additional random noise from motion of fringes in the spectrum relative to the HNO_3 line positions. We find that the sensitivity-limiting noise corresponds to 150-200 ppt of HNO_3 . However, this noise is random, and thus uncorrelated with the atmospheric eddies carrying fluxes into the forest canopy. We can therefore average the covariance of HNO_3 and w over the ensemble averaging period (30 min) for forest flux observations²³. An estimate of the precision for the 30-minute flux is obtained by using the relationship between covariance, the standard deviation of measured quantities, and the correlation coefficient:

$$\text{covariance} = \sigma(\text{HNO}_3) \sigma(w) r(w, \text{HNO}_3) \quad (1)$$

The peak of a representative power spectrum, $r(w, \text{NO}_y)$ at Harvard Forest is approximately 0.15⁸. A random sampling (days 15, 115, 215, and 315) of the Harvard Forest 1996 data set indicates that $\sigma(w)$ is roughly 0.1 ms^{-1} for low momentum flux conditions where a near-zero HNO_3 flux is expected. We therefore estimate the HNO_3 flux precision to be less than or equal to 2 ppt m s^{-1} , equivalent to $0.3 \mu\text{ moles m}^{-2} \text{ hr}^{-1}$. This is the 15th percentile (or better) for fluxes of NO_y at Harvard Forest⁷.

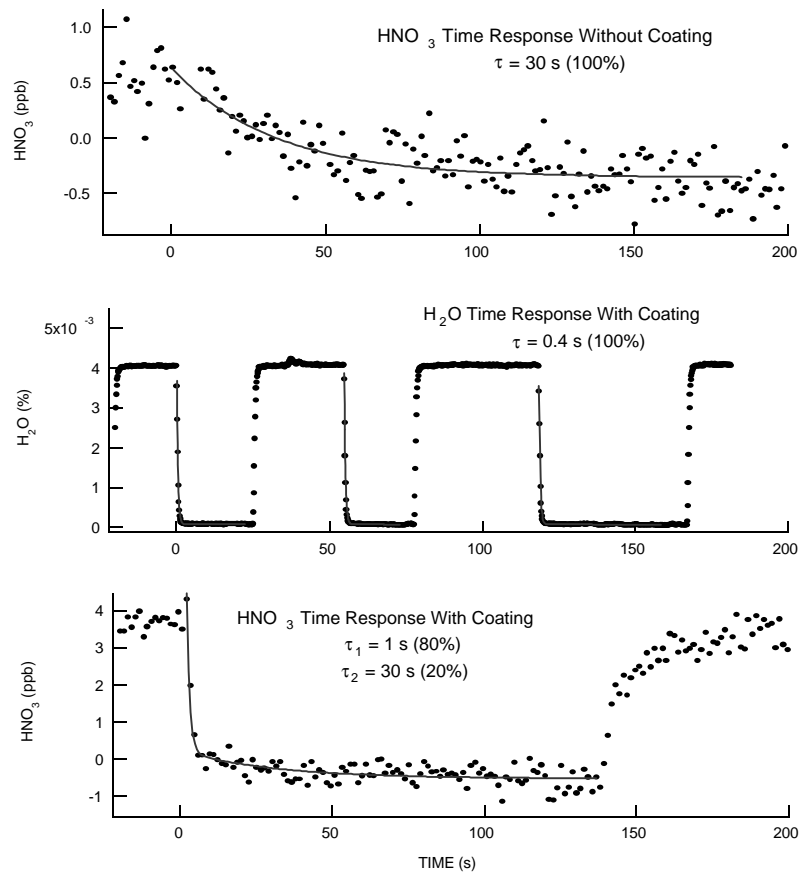


Figure 4. Upper panel: Response to HNO_3 with uncoated pyrex flow tube. Center panel: Response water vapor with siloxyl-coated pyrex flow tube. Lower panel: Response to HNO_3 signal with coated pyrex flow tube. In each case, the fit (line) = $A \exp(-t/\tau_1) + B \exp(-t/\tau_2)$.

2.3. Measurement of NO₂

The TDLAS technique has been applied successfully to nitrogen oxide emissions detection, demonstrating the sensitivity and suitability of the method^{24,25}. Atmospheric measurements of NO₂, like HNO₃, require a combination of strong absorption features in spectral regions where there is minimal interference from other absorbing species. Optimal spectral regions for NO₂ detection at 1600 cm⁻¹, part of the ν_3 asymmetric stretch mode, give line center fractional absorbances of approximately 4×10^{-6} for 10 ppt NO₂ using the 210 m pathlength cell configuration. One-second, integrated measurements of both zero air and a constant NO₂ permeation tube source show that the RMS noise at all levels is 80 ppt over the 210 m path. Figure 5 shows an experimental NO₂ spectrum with a non-linear least squares fit.

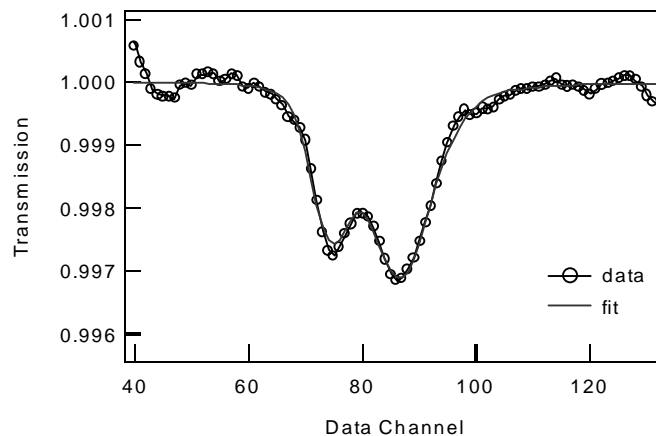


Figure 5. NO₂ spectrum, 1599.8 cm⁻¹ to 1600 cm⁻¹, sampled in indoor ambient air. The fingerprint fit corresponds to 7.1 ppb NO₂.

NO and NO₂ cycle rapidly in response to gradients in O₃ concentration and light intensity through the forest canopy. This may lead to apparent exchange of NO₂ when in fact there is no net flux of NO_x. The contribution of NO/NO₂ cycling can be separated from true NO_x exchange (NO₂ deposition or NO emission) by making continuous measurements of NO, NO₂, and O₃ concentrations, and covariances of NO, NO_y, O₃, and T with w ²⁶. Since the NO, NO_y, and O₃ detectors are located at the main Harvard Forest flux tower approximately 100 m from the TDLAS flux tower, we will also collocate a fast-response NO sensor with the TDLAS inlet for a validation period.

3. FIELD DEPLOYMENT

3.1. Pilot Field Measurements

A preliminary intercomparison using an early prototype of the TDLAS HNO₃ monitor allowed for validation of the measurement technique as well as identification of a number of technical problems, which have now been solved. Field measurements of HNO₃ were conducted at the NOAA Aeronomy Laboratory (AL) Enchanted Mesa site approximately 3 km southwest and 100 m above Boulder, CO from October 13 through November 5, 1996. Three methods were used to measure atmospheric HNO₃: the NOAA AL CIMS^{11,27}, the NOAA Filter Pack (FP) method, and the ARI prototype TDLAS. The two fast-response instruments (CIMS and TDL) were housed in side-by-side trailers so that the inlets were approximately 3 m apart and 2 m off the ground, each inlet extending horizontally from the west end of the trailers. The FP measurements represent a more established, long integration time technique providing a point of reference for the other, newer methods. Figure 6 shows the diurnal average of HNO₃ measured by the CIMS and TDL during the intercomparison period.

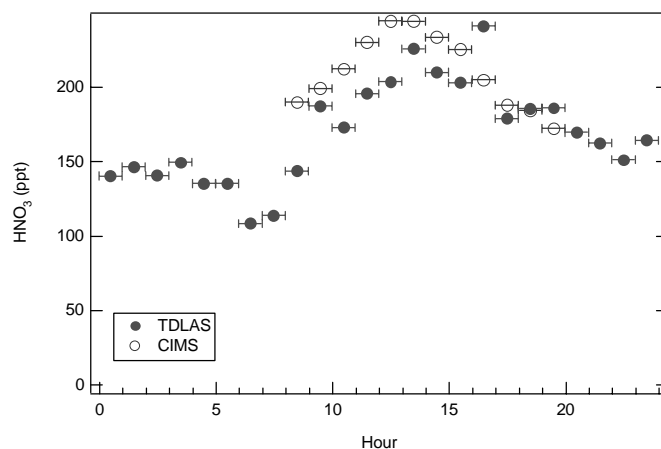


Figure 6. Average diurnal cycles of HNO₃ over the intercomparison period in hourly bins. Nighttime TDLAS data was acquired in an unattended mode.

The HNO₃ TDLAS prototype differed from the current Harvard-Aerodyne instrument in its lack of temperature control, lower reflectivity mirrors, correspondingly higher detection limit and noise characteristics, and lower duty cycle. Despite the noise present in the TDL system, the spectroscopic measurement technique allowed for unambiguous identification of HNO₃.

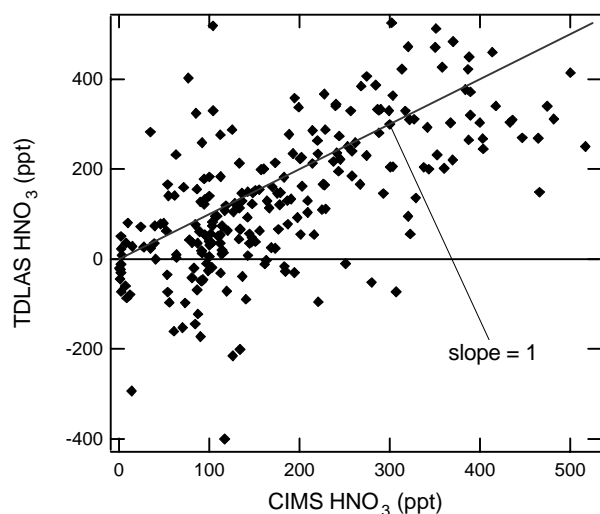


Figure 7. Comparison of TDLAS and CIMS HNO_3 measurements from Enchanted Mesa, Colorado as 10-minute average data points. The slope of the linear regression is 0.85 ± 0.06 , and the intercept is at -20 ± 13 ppt. $R^2 = 0.45$.

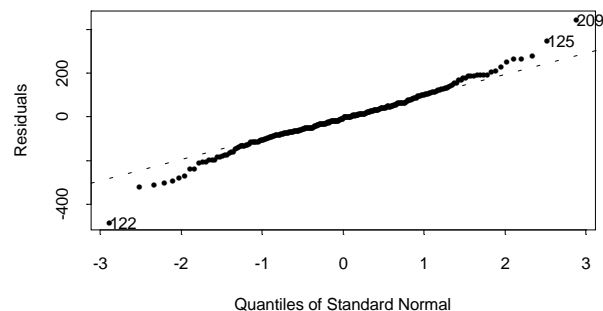


Figure 8. Residuals of the linear regression to data in the previous figure, plotted against quantiles of the standard normal. Points fall predominantly on a straight line, indicating that the excess noise in the TDLAS data is Gaussian in nature.

In Figure 3, signal and background spectra from a 6-hour sampling period during the intercomparison have been co-averaged and then ratioed to produce a high signal to noise HNO_3 spectrum. The peak fractional absorption is 3×10^{-5} , corresponding to a nitric acid concentration of 149 ppt. The agreement between spectra co-averaged over hour-long periods and hourly averages of the real-time HNO_3 measurements made by the TDL was excellent, indicating the certainty with which the TDL technique is able to identify and measure the HNO_3 present in the long-path sampling cell. TDL measurements from the prototype hourly-average detection limit of 20 ppt up to 500 ppt HNO_3 were observed during the Colorado field campaign. This wide range of values is typical of the site, which samples very clean, westerly flow from over the mountains as well as polluted, easterly flow from the Denver metropolitan area.

Figure 7 shows all concurrent CIMS and TDLAS measurements during the intercomparison period as 10-minute average data points. The two methods are in good agreement overall. Unlike the CIMS, the TDLAS is allowed to report negative concentrations. These values represent instances when the background and signal spectra no longer represent the same conditions in the cell, usually due to temperature drifts in the unregulated prototype. The negative concentrations are the best solutions to the least-squares fits of the invalid spectra. Figure 8 displays residuals of the linear regression against quantiles of the standard normal. The occurrence of most of the residuals on the straight line indicates that the TDLAS noise is normally distributed, revealing no pronounced systematic or non-random discrepancy between the data sets. The two different techniques agree under a wide range of conditions. Although the TDL prototype's lack of active temperature control, higher detection limit, and low duty cycle were the limiting factors in extracting more detailed information from the data set, the good agreement between the spectroscopic, absolute method and the calibration-based CIMS technique was an important step in the development of both approaches.

3.2. Harvard Forest Deployment

The Harvard Forest site in central Massachusetts (42.54N, 72.18W; elevation, 340 m) is a 50- to 70-year old mixed deciduous forest consisting primarily of red oak and red maple, with scattered hemlock, red pine, and white pine stands. The terrain is roughly 95% forested and moderately hilly; closest paved roads are more than 1 km away, small towns greater than 10 km distant. Dominant winds are from the northwest and southwest. The 30 m tower on which the current suite of measurements is based rises 6-10 m above the forest canopy.

The dual TDLAS will measure HNO_3 and NO_2 concentrations and fluxes on a walk-up tower approximately 100 m from the main flux tower during a one-year period, beginning in the summer of 1999. The instrument is at a height of 20 m, with a 3

m inlet extension added so that the sampling level is approximately 110% of the canopy height. The coated quartz inlet extension samples an excess flow at atmospheric pressure such that concentration fluctuations relevant to turbulent transport are preserved and fewer than 20% of the molecules have interacted with the walls by the time they enter the multipass cell inlet^{28,29}. The inlet extension introduces a finite lag time between the sonic anemometer wind field and the TDLAS concentration measurements. A routine correction is made for the lag time when the flux is calculated using observed lagged cross-correlations³⁰.

A Campbell Scientific sonic anemometer is installed on the same tower as the TDLAS instrument at the same height as the inlet extension. Auxiliary equipment, such as control and data acquisition electronics, is installed in a shed at the base of the tower along with pumps and gas cylinders. The electronics module and liquid nitrogen supply are on the tower, one stage below the main optics module in order to minimize the cable length between the lasers and the diode laser controller. The data control and acquisition program running at the base of the tower is interfaced with the Campbell Scientific CR10x datalogger via short-haul modem. The sonic anemometer data is routinely scanned for noise spikes, as indicated by the ratios between σ_w , σ_u , σ_v , and u^* . The virtual temperature derived from the speed of sound will also be compared with thermistor temperature measurements to eliminate data taken with water on the sonic transducers, as is presently done for all Harvard Forest sonic anemometer data.

Data from a continuous one-year period will be used to investigate the role of the reactive nitrogen budget in tropospheric ozone production. Measurements of HNO_3 and NO_2 , along with PAN, NO and NO_y measurements will provide nearly complete NO_y speciation so that the partitioning of reactive nitrogen will be better understood for this continental site. Fluxes of HNO_3 and NO_2 will provide direct quantitative information on reactive nitrogen loss processes, which directly effect ozone production. This data set will be investigated in the context of measurements of NO_y and O_3 fluxes, as well as NO_x , hydrocarbon, and tracer concentrations for meaningful correlations revealing photochemical and transport processes important in the boundary layer nitrogen budget and ozone production. The sum of individual nitrogen oxide species measured at the site, including NO, NO_2 , PAN, and HNO_3 can be compared with the independent NO_y measurement to evaluate the portion of NO_y composed of unknown or unmeasured species. This comparison will also be an important check on the validity of all the nitrogen oxide measurements, providing an indicator for unforeseen interferences. Inspection of cospectra of $w'\text{HNO}_3'$ and $w'\text{NO}_2'$ compared to $w'T'$ will reveal any incomplete resolution of small eddies.

4. CONCLUSION

The dual TDLAS has demonstrated the high sensitivity and fast time response required for measuring eddy covariance fluxes of HNO_3 and NO_2 to forest ecosystems. The long-path astigmatic Herriot cell with narrow-band IR mirror coatings and multiplexed beams provides sufficient pathlength and light throughput to routinely detect fractional absorptions on the order of 10^{-5} in a 1 second measurement. Along with maintaining a constant pressure in the absorption cell, active temperature control of the entire optical table and enclosure stabilizes interference fringes with respect to line positions. This design feature extends the time between required background spectra, thus raising the duty cycle for atmospheric measurements to better than 80%. Efficient sampling of HNO_3 has been achieved by keeping wall contact to a minimum and using coated Pyrex and quartz surfaces with favorable responses to this highly polar molecule.

The measurements at Harvard Forest will test ideas about mechanisms controlling partitioning among of nitrogen oxide species and their ultimate removal from the atmosphere. The observations will produce new information on seasonal and interannual variability in the reactive nitrogen budget, and quantify an important component of acid deposition to forest ecosystems. The major questions to be addressed are:

- 1) What are the magnitudes of the deposition fluxes of NO_2 and HNO_3 at forested sites in New England?
- 2) Is HNO_3 the major species that contributes to dry deposition of NO_y ?
- 3) Does deposition of NO_2 to the forest canopy have a significant effect on tropospheric ozone production and on the oxidizing potential of atmospheric NO_x ?

ACKNOWLEDGMENTS

Support for this project has been provided by the NOAA Global Change, NSF SBIR, and NASA SBIR programs at Aerodyne Research, Inc. and by the Merck Foundation at Harvard University. The authors thank L. Gregory Huey and Fred C. Fehsenfeld for their CIMS HNO_3 measurements and for coordinating the 1996 intercomparison. Bruce C. Daube, Alfram V.

Bright (Harvard), Robert Prescott, and Jeff Mulholland (ARI) are gratefully acknowledged for their contributions to the design, construction, and deployment of the dual TDLAS instrument. The authors also thank J. William Munger for his continuing investigations of reactive nitrogen chemistry at Harvard Forest.

REFERENCES

1. J. A. Logan, "Nitrogen oxides in the troposphere: Global and regional budgets," *J. Geophys. Res.*, *88*, 10,785-10,807, 1983.
2. P. Crutzen, "The role of NO and NO₂ in the Chemistry of the Troposphere and Stratosphere," *Ann. Rev. Earth. Planet. Sci.* *7*, 443-472, 1979.
3. B. A. Ridley and E. Robinson, "The Mauna Loa Observatory Photochemistry Experiment," *J. Geophys. Res.*, *97*, 10,285-10,290, 1992.
4. R. W. Talbot, A. S. Vijgen, and R. C. Harriss, "Soluble Species in the Arctic Summer Troposphere: Acid Gases, Aerosols, and Precipitation," *J. Geophys. Res.*, *97*, 16,531-16,543, 1992.
5. H. B. Singh et al., "Reactive nitrogen and ozone over the western Pacific: Distribution, partitioning, and sources," *J. Geophys. Res.*, *101*, 1793-1808, 1996.
6. J. A. Logan, M. J. Prather, S. C. Wofsy, and M. B. McElroy, "Tropospheric chemistry: A global perspective," *J. Geophys. Res.*, *86*, 7210-7254, 1981.
7. J. W. Munger, S.-M. Fan, P. S. Bakwin, M. L. Goulden, A. H. Goldstein, A. S. Colman, and S. C. Wofsy, "Regional budgets for Nitrogen Oxides from Continental Sources: Variations of rates for oxidation and deposition with season and with distance from source regions," *J. Geophys. Res.*, *103*, 8355-8368, 1998.
8. J. W. Munger, S. C. Wofsy, P. S. Bakwin, S.-M. Fan, M. L. Goulden, B. C. Daube, and A. H. Goldstein, "Atmospheric deposition of reactive nitrogen oxides and ozone in a temperate deciduous forest and a subarctic woodland," *J. Geophys. Res.*, *101*, 12,639-12,657, 1996.
9. R. W. Talbot, A. S. Vijgen, and R. C. Harriss, "Measuring Tropospheric HNO₃: Problems and Prospects for Nylon Filter and Mist Chamber Techniques," *J. Geophys. Res.*, *95*, 7553-61, 1990.
10. B. L. Lefer, R. W. Talbot, and J. W. Munger, "Nitric acid and ammonia at a rural northeastern U.S. site," *J. Geophys. Res.*, *104*, 1645-1661, 1999.
11. L. G. Huey, E. J. Dunlea, E. R. Lovejoy, D. R. Hanson, R. B. Norton, F. C. Fehsenfeld, C. J. Howard, "Fast Time Response Measurements of HNO₃ in Air with a Chemical Ionization Mass Spectrometer," *J. Geophys. Res.* *103*, 3355-60, 1998.
12. R. L. Mauldin III, D. J. Tanner, F. L. Eisele, "A new chemical ionization mass spectrometer technique for the fast measurement of gas phase nitric acid in the atmosphere," *J. Geophys. Res.*, *103*, 3361-7, 1998.
13. T. M. Miller, J. O. Ballenthin, R. F. Meads, D. E. Hunton, W. F. Thorn, and A. A. Viggiano, "CIMS technique for the measurement of HNO₃ in air traffic corridors in the upper troposphere during the SONEX campaign," submitted to *J. Geophys. Res.*, 1999.
14. R. W. Talbot, J. E. Dibb, E. M. Scheuer, Y. Kondo, M. Koike, H. B. Singh, L. B. Salas, A. A. Viggiano, J. O. Ballenthin, T. M. Miller, D. R. Blake, N. J. Blake, E. Atlas, F. Flocke, D. J. Jacob, and L. Jaegle, "Reactive nitrogen budget during the NASA SONEX mission," Submitted to *Geophys. Res. Lett.*, 1999.
15. Singh, H. B. et al., "Reactive nitrogen and ozone over the western Pacific: Distribution, partitioning, and sources," *J. Geophys. Res.*, *101*, 1793-1808, 1996.
16. S. Sandholm et al., "Summertime partitioning and budget of NO_y compounds in the troposphere over Alaska and Canada: ABL3B," *J. Geophys. Res.*, *99*, 1837-1861, 1994.
17. M. S. Zahniser, D. D. Nelson, J. B. McManus, and P. L. Keenan, "Measurement of trace gas fluxes using tunable diode laser spectroscopy," *Philosophical Transactions of the Royal Society*, *A351*, 371-382, 1995.
18. H. I. Schiff, D. R. Kerecki, G. W. Harris, D. R. Hastie, and G. I. Mackay, "A Tunable Diode Laser System for Aircraft Measurements of Trace Gases," *J. Geophys. Res.*, *95*, 10,147-53, 1990.
19. D. D. Nelson, M. S. Zahniser, J. B. McManus, and J. H. Shorter, "Recent improvements in atmospheric trace gas monitoring using mid-infrared tunable diode lasers," *Proc. SPIE* *2834*, 148-159, 1996.
20. K. A. Boering, B. C. Daube, S. C. Wofsy, Jr., M. Loewenstein, J. R. Podolske, and T. J. Conway, "Stratospheric transport rates and mean age distribution derived from observations of atmospheric CO₂ and N₂O," *Science*, *274*, 1130-1134, 1996.
21. J. B. McManus, P. L. Keenan, and M. S. Zahniser, "Astigmatic mirror multiple pass absorption cells for long pathlength spectroscopy," *Appl. Opt.*, *34*, 3336, 1995.

-
22. L. S. Rothman et al., "The HITRAN molecular spectroscopic database and HAWKS (HITRAN Atmospheric Workstation): 1996 Edition," *J. Quant. Spectrosc. Radiat. Transfer*, 60, 665-710, 1998.
 23. D. H. Lenschow and L. Kristensen, "Uncorrelated noise in turbulence measurements," *J. Atmos. Ocean. Tech.*, 2, 1, 68-81, 1985.
 24. D. D. Nelson, M. S. Zahniser, J. B. McManus, C. E. Kolb, and J. L. Jimenez, "A tunable diode laser system for the remote sensing of on-road vehicle emissions," *Appl. Phys. B* 67, 433-441, 1998.
 25. J. Wormhoudt, M. S. Zahniser, D. D. Nelson, J. B. McManus, R. C. Miale-Lye, and C. E. Kolb, "Infrared tunable diode laser measurements of nitrogen oxide species in an aircraft engine exhaust," *Proceedings SPIE 2546*, 552-561, 1995.
 26. D. R. Fitzjarrald and Lenschow, D. H., "Mean concentration and flux profiles for chemically reactive species in the atmospheric surface layer," *Atmos. Environ.* 17, 2505-2512, 1983.
 27. F. C. Fehsenfeld, L. G. Huey, D. Sueper, D. Norton, E. Williams, F. Eisele, L. Mauldin, D. Tanner, Ground-based intercomparison of nitric acid measurement techniques, *J. Geophys. Res.*, 103, 3343-53, 1998.
 28. D. H. Lenschow and M. R. Raupach, "The attenuation of fluctuations in scalar concentrations through sampling tubes," *J. Geophys. Res.* 96, 15259-68, 1991.
 29. W. J. Massman, "The attenuation of concentration fluctuations in turbulent flow through a tube," *J. Geophys. Res.* 96, 16269-73, 1991.
 30. M. L. Goulden, J. W. Munger, S.-M. Fan, B. C. Daube, and S. C. Wofsy, "Measurements of carbon sequestration by long-term eddy covariance: methods and a critical evaluation of accuracy," *Global Change Bio.*, 2, 169-182, 1996.